

Subject: Soils -- Geophysical Assistance

Date: 31 October 2006

To: David Hoover
State Soil Scientist
USDA-NRCS
9173 West Barnes Drive, Suite C
Boise, ID 83709

Dr. Paul A. McDaniel
Professor of Soil Science
Soil & Land Resources Division
University of Idaho
P.O. Box 442339
Moscow, Idaho 83844-2339

Purpose:

Abrupt and well defined divisions exist between vegetated and non-vegetated areas on cinder flats and cones within Craters of the Moon National Monument and Preserve. On 40-year old photography, these boundaries appear to maintain the same position without any advancement or retreat on cinder cones and flats. The purpose of this investigation was to use GPR to investigate these boundaries and identify subsurface features that would promote these divisions and differences. In addition, GPR surveys were conducted in areas of medium-textured soils formed in aeolian deposits over basalt within Craters of the Moon National Monument and in an area of Dune land within the Saint Anthony Dune Field.

Principal Participants:

John Apel, Intergrated Resource Program Manager, USDI-NPS, Craters of the Moon National Monument and Preserve, Arco, ID

Karen Castenson, PhD Candidate, College of Ag and Life Sciences, Univ. of Idaho, Moscow, ID

Jim Doolittle, Research Soil Scientist, USDA-NRCS-NSSC, Newtown Square, PA

Rod Kyar, Soil Scientist, USDA-NRCS, Boise, ID

Bob Kukachka, Soil Scientist, USDA-NRCS, Soda Springs, ID

Glenn Hoffmann, Soil Scientist, USDA-NRCS, Idaho Falls, ID

Bill Hiatt, Soil Scientist, USDA-NRCS, Idaho Falls, ID

Dave Hoover, State Soil Scientist, USDA-NRCS, Boise, ID

Paul McDaniel, Professor of Soil Science, College of Ag and Life Sciences, Univ. of Idaho, Moscow, ID

Hal Swenson, Soil Scientist, USDA-NRCS, Boise, ID

Activities:

All field activities were completed during the period of 17 to 19 October 2006.

Summary:

1. A goal of this investigation was to use GPR to identify subsurface stratigraphic features that would promote the development of vegetation on cinders. Investigated cinder lands sites within Craters of the Moon National Monument and Preserve were well suited to GPR. Subtle differences were noted between barren and vegetated areas on radar records. These differences are attributed to the affects of vegetation on soil development. However, GPR surveys provided little evidence that would support

vegetation developing on stratigraphically different materials.

2. Electromagnetic induction revealed higher apparent conductivity (EC_a) in surface layers of vegetated areas than over barren cinders. This relationship is attributed to the thin mantle of soil within the vegetated areas. The higher EC_a is inferred to result from the soil mantle having higher organic matter, clay, and moisture contents than the cinders.
3. In areas of Deerhorn and Rehfield soils, relatively high clay and calcium carbonate contents severely attenuated the radars energy and restricted penetration depths. High levels of background noise plagued radar records, and ambiguous and poorly resolved reflections limited interpretations. These adverse conditions necessitated the use of advance computer processing techniques, which resulted in only minor improvements in interpretations. In areas where the bedrock was deeper than 100 cm, it was generally indiscernible. The use of GPR is considered inappropriate for most soil survey investigations on soils formed in calcareous aeolian deposits over basalt soils.
4. At the Saint Anthony Dune Field, GPR records revealed the internal geometry and structure of major stratigraphic boundaries within a low dune. With a 200 MHz antenna, depths of penetration varied from 1.2 to 7.0 m. The depth of penetration appears to be limited mostly by the specific conductance of the groundwater.

As always, it is my pleasure to work in Idaho, with your staff and with Paul McDaniel and Karen Castenson.

With kind regards,

James A. Doolittle
 Research Soil Scientist
 National Soil Survey Center

cc:

- B. Ahrens, Director, National Soil Survey Center, USDA-NRCS, Federal Building, Room 152, 100 Centennial Mall North, Lincoln, NE 68508-3866
- K. Castenson, PhD Candidate, College of Ag & Life Sciences, P.O. Box 442339, Moscow, Idaho 83844-2339
- M. Golden, Director of Soils Survey Division, USDA-NRCS, Room 4250 South Building, 14th & Independence Ave. SW, Washington, DC 20250
- G. Hoffman, Soil Scientist, USDA-NRCS, 1120 E Lincoln Rd., Idaho Falls, ID 83401-2122
- D. Hoover, State Soil Scientist, USDA-NRCS, 9173 West Barnes Drive, Suite C, Boise, ID 83709-1574
- D. Hammer, National Leader, Soil Investigation Staff, USDA-NRCS, National Soil Survey Center, Federal Building, Room 152, 100 Centennial Mall North, Lincoln, NE 68508-3866
- F. Kukachka, Soil Scientist, USDA-NRCS, 390 E Hooper Ave., Soda Springs, ID 83276-1443
- C. McGrath, MLRA Office Leader, USDA-NRCS, 1201 NE Lloyd Blvd., Suite 900, Portland, OR 97232
- W. Tuttle, Soil Scientist (Geophysical), USDA-NRCS-NSSC, P.O. Box 974, Federal Building, Room G08, 207 West Main Street, Wilkesboro, NC 28697

Background:

Ground-penetrating radar (GPR) has been used extensively to characterize the distribution, composition, internal features, thickness, and volume of volcanic deposits (Gomez-Ortiz et al., 2006; Grimm et al., 2006; Heggy et al., 2006; Shapiro et al., 2005; Miyamoto et al., 2003; Olhoeft et al., 2000; Russell and Stasiuk, 2000 & 1997; Gilbert et al., 1996; and McCoy et al., 1992). Gomez-Ortiz et al. (2006) evaluated the performance of GPR in several volcanic materials (massive lava flows, pahoehoe and a 'a lava flows, and airfall deposits). Rust and Russell (2001) used GPR to map porosity variations in pyroclastic flow deposits from the eruption of Mount Mazama, in south-central Oregon. Rust and Russell (2001) noted that subsurface reflectors were generally well defined in pahoehoe, but poorly defined in a 'a lava flows. Miyamoto et al. (2003) and Olhoeft et al. (2000) used GPR to investigate lava tubes.

In general, volcanic deposits have been found to be well suited to GPR. These deposits are comparatively homogenous in composition and electrically resistive (Russell and Stasiuk, 1997). Differences in composition of volcanic deposits have been recognized based on differences in signal attenuation and radar reflection patterns (Rust and Russell, 2001).

While GPR has been used extensively on volcanic deposits, much remains unknown. The depth of penetration and the effectiveness of GPR in different volcanic materials have not been fully assessed and the results of some studies appear contradictory. Very restricted penetration depths have been reported in volcanic soils of arid regions (Paillou et al., 2001). In arid regions, restricted penetration depths are associated with high concentrations of ferromagnetic materials, calcium carbonates, evaporates (halite), and gypsum in the soils formed from basalt. Greater rates of signal attenuation and restricted penetration depths are attributed to strong conduction and relaxation losses in these soils (Paillou et al., 2001).

In studies performed directly over volcanic materials, and in the absence of soil materials, exceptional penetration depths have been achieved with GPR. Russell and Stasiuk (2000) used a low frequency (50 MHz) antenna to estimate the thickness of individual pyroclastic (ash, pumice, and lapilli) units to depths of 18 to 20 m. Though the radar imagery is poor and results ambiguous and highly interpretative, penetration depths as great as 55 m were reported in pumice (Russell and Stasiuk, 1997). Grimm et al. (2006) reported penetration depths of 4 to 14 m in welded tuff. In a study conducted at Craters of the Moon National Monument and Preserve, Heggy et al. (2006) reported penetration depths as great as 35 m and 80 m with 100 and 16 MHz antennas, respectively. These reported depths are considered exceptional. Heggy et al. (2006) observed that for frequencies below 100 MHz, signal loss was dominated by electromagnetic attenuation. However, for frequencies above 100 MHz scattering losses caused by heterogeneities in the volcanic materials were more significant.

Areas of Cinder land and soils developed from cinders are considered well suited to GPR. The purpose of this study was to use relatively high frequency (400 and 900 MHz) antennas to identify features in the upper 1 to 3 meters of soils and cinder deposits that would influence the observed differences in vegetative patterns.

Study Sites:

Two sites were selected in the northern part of Craters of the Moon National Monument and Preserve. These sites are referred to as the *Cinder Garden Site* and the *Service Road Site*. Parent materials consist of volcanic ejecta. The *Cinder Garden Site* is located on a cinder flat that is adjacent to the Loop Road between Paisley and Inferno Cones. The *Cinder Garden Site* is in areas of Cinder land-Northcrater association, 2 to 50 percent slopes (map unit (MU) 7) and Bigcinder ashy sandy loam, 20 to 40 percent slopes (MU 3). The *Service Road Site* is located on an unidentified cinder cone near the Monument's campground. The *Service Road Site* is in an area of Echocrater gravelly ashy loamy sand, 20 to 40 percent slopes (MU 15). The very deep, well drained Bigcinder and Echocrater soils formed in volcanic ash and cinders. The very deep, excessively drained Northcrater soils formed in volcanic tephra. These soils lack carbonates and soluble salts, and have less than 6 percent clay throughout (<http://soildatamart.nrcs.usda.gov/>). Depth to 2C horizon, which contains 90 to 100 percent cinders, ranges from 5 to 25 inches. These chemical and physical properties are favorable to GPR. These soils are rated as being well suited to GPR on the GPR Soil Suitability Map of Idaho (see

<http://soils.usda.gov/>). Miscellaneous areas of Cinder land are not currently rated for GPR, but should be regarded as being well suited.

Table 1
Soil Series traversed with GPR at Craters of the Moon National Monument and Preserve

| <u>Series</u> | <u>Taxonomic Classification</u> |
|---------------|---|
| Bigcinder | Ashy-skeletal over fragmental or cindery, aniso, glassy Xeric Vitricryands |
| Echocrater | Ashy-skeletal over fragmental or cindery, glassy, frigid Typic Vitrixerands |
| Northcrater | Ashy-skeletal, glassy, nonacid, frigid Vitrandic Xerorthents |

Table 1 lists the taxonomic classifications of the soils at the study sites. Soils at the Cinder Garden and Service Road sites were sampled and classified by (Dr. Paul McDaniel and Karen Castenson) as pumiceous, amorphic Xeric Vitricryands and as pumiceous, glassy Xeric Vitricryands, respectively.

Equipment:

The radar unit is the TerraSIRch Subsurface Interface Radar (SIR) System-3000, manufactured by Geophysical Survey Systems, Inc. (Salem, New Hampshire).¹ Daniels (2004) discusses the use and operation of GPR. The SIR System-3000 weighs about 9 lbs (4.1 kg) and is backpack portable. With an antenna, the system requires two people to operate. The 200, 400, and 900 MHz antennas were used in this investigation.

Radar records contained in this report were processed with the RADAN for Windows (version 5.0) software program developed by Geophysical Survey Systems, Inc.¹ Processing included setting the initial pulse to time zero, color transformation, marker editing, distance normalization, horizontal stacking, background removal, migration, and range gain adjustments. Surface normalization was applied to the GPR data from the Saint Anthony Dune Field site where elevation data had been collected along the traverse line.

An EM38DD electrical conductivity meter was used at the *Cinder Garden Site*, at Craters of the Moon National Monument and Preserve. The EM38DD meter is manufactured by Geonics Limited (Mississauga, Ontario).¹ Operating procedures for the EM38DD meter are described by Geonics Limited (2000). This meter is portable and requires only one person to operate. The EM38DD meter has a 1-m intercoil spacing and operates at a frequency of 14,600 Hz. When placed on the soil surface, the EM38DD meter provides theoretical penetration depths of about 0.75 and 1.5 m in the horizontal and vertical dipole orientations, respectively. No ground contact is required with this device. Lateral resolution is approximately equal to the intercoil spacing. Electromagnetic induction (EMI) meters measure the apparent conductivity (EC_a) of earthen materials. Apparent conductivity is expressed in milleSiemens per meter (mS/m).

Geonics' DAS70 Data Acquisition System (developed by Geonics Limited) was used with EM38DD meter to record and store both EC_a and Global Positioning System (GPS) data.¹ The acquisition system consists of the EM38DD meter, an Allegro field computer (Juniper Systems, North Logan, Utah), and a Garmin Global Positioning System Map 76 receiver (with a CSI Radio Beacon receiver, antenna, and accessories that are fitted into a backpack) (Olathe, KS).¹ With the acquisition system, the EM38DD meter is keypad operated and measurements are automatically triggered.

To help summarize the results of the EMI survey, SURFER for Windows (version 8.0) software, developed by Golden Software, Inc. (Golden, Colorado), was used to construct two-dimensional simulations.¹ Grids were created using kriging methods with an octant search.

Survey Procedures:

¹ Manufacturer's names are provided for specific information; use does not constitute endorsement.

Multiple GPR traverse lines were established at both sites within the Craters of the Moon National Monument and Preserve. The length of these traverse lines varied with vegetative conditions and accessibility. Each traverse line began on a cinder barren and entered a vegetative zone. Along each line, reference points were spaced at 1 meter intervals. As the radar antenna was pulled passed each reference point, a mark was inserted on the radar record. Eleven GPR traverse lines were established at the *Cinder Garden Site* and five GPR traverse lines were established at the *Service Road Site*. The end points of these traverse lines were recorded with the GPS. However, these files were corrupted and lost. Table 2 lists the length and the location of the vegetated area along of each traverse line. The locations of the vegetated areas are referenced to the distance marks (reference points) along each GPR traverse line. These distances are measured in meters from the beginning of each traverse line. For the *Service Road Site*, Line 2 had a noticeable barren area included within the vegetated area between distance marks 10 to 12 m.

A *random walk* or *wild-cat* EMI survey was conducted with the EM38DD meter at the *Cinder Garden Site*. The EM38DD meter was operated in continuous mode with measurements recorded at 1-sec intervals. The meter was held about 3 cm (about 1 inch) above the ground surface in barren areas and frequently, slightly higher in vegetated areas. The meter was orientated with its long axis parallel to the direction of traverse. The EMI survey was completed by walking at a rather slow and uneven pace, in a random pattern across the more accessible portions of survey area. The survey was obstructed by plants and litter in portions of the vegetative areas.

Table 2
GPR Traverse Lines at Craters of the Moon National Monument and Preserve

| <i>Cinder Garden Site</i> | | |
|---------------------------|-------------------|---------------------------|
| <u>Line #</u> | <u>Length (m)</u> | <u>Vegetated Area (m)</u> |
| 0 | 40 | 13 to 32 |
| 1 | 25 | 10 to 21 |
| 2 | 24 | 12+ |
| 3 | 20 | 11+ |
| 4 | 25 | 12+ |
| 5 | 20 | 11+ |
| 6 | 25 | 9+ |
| 7 | 20 | 12+ |
| 8 | 20 | 10+ |
| 9 | 15 | --- |
| 10 | 43 | 21 to 33 |

| <i>Service Road Site</i> | | |
|--------------------------|-------------------|---------------------------|
| <u>Line #</u> | <u>Length (m)</u> | <u>Vegetated Area (m)</u> |
| 1 | 12 | 8+ |
| 2 | 14 | 7+ |
| 3 | 18 | 11+ |
| 4 | 13 | 8+ |
| 5 | 13 | 7+ |

Calibration of GPR:

Ground-penetrating radar is a time scaled system. This system measures the time that it takes electromagnetic energy to travel from the antenna to an interface (e.g., bedrock, soil horizon, stratigraphic layer) and back. To

convert the travel time into a depth scale, either the velocity of pulse propagation or the depth to a reflector must be known. The relationships among depth (D), two-way pulse travel time (T), and velocity of propagation (v) are described in the following equation (Daniels, 2004):

$$v = 2D/T \quad [1]$$

The velocity of propagation is principally affected by the relative dielectric permittivity (E_r) of the profiled material(s) according to the equation:

$$E_r = (C/v)^2 \quad [2]$$

where C is the velocity of propagation in a vacuum (0.298 m/ns). Velocity is expressed in meters per nanosecond (ns). In soils, the amount and physical state of water (temperature dependent) have the greatest effect on the E_r and v .

Based on the known depth to a buried reflector and hyperbola-matching processing techniques (the shape of a hyperbole is dependent on signal velocity), the velocity of propagation through the upper part of the soil was determined. With the 400 MHz antenna, the estimated E_r was 3.89 and the v was 0.151 m/ns. This information was used to depth scale the radar records. As the velocity of propagation is spatial variable, depth scales are close approximations, but are not exact.

Results:

GPR Surveys at Craters of the Moon National Monument and Preserve:

Ground-penetrating radar is well suited for use on soils formed from cinders. For soil investigations spanning depths of 1 to 3 m, the 400 MHz antenna provides the best balance of penetration depth and resolution. The 900 MHz antenna is best suited to shallow (0 to 50 cm) and moderately deep (50 to 100 cm) investigations, but suffers from higher levels of attenuation and scattering losses. Radar records collected with the 900 MHz antenna were generally less clear and interpretable than those collected with the 400 MHz antenna. In cinders, scattering losses and background noise can be reduced by using lower frequency antennas.

Figure 1 is a 22-m portion of traverse line 2 at the *Cinder Garden Site*. This record was obtained with the 400 MHz antenna. In Figure 1, all scales are in meters. The 400 MHz has provided highly resolved images of the subsurface to a depth of about 3.5 m. However, this is not the maximum depth of penetration attainable with the 400 MHz antenna in areas of Cinder lands, and Northcrater and Bigcinder soils. Had the range been increased, deeper depths could have been achieved.

The first 12-m of the radar traverse line (see Figure 1) was conducted across barren cinders. A vegetated area was entered near the 12-m mark and extends to the end of the traverse line. High amplitude (identified by white, pink and gray colors) surface reflections and reverberations are evident in the upper 10 to 40 cm for the first 12 to 13 meters of this radar record. These reflections are produced by the comparatively hard and dense cinder surface. In the last 10 meters (distance marks 12 to 22-m) of this GPR traverse, the surface reflections and reverberations are more variable in expression and consist of moderate amplitudes (identified by blue, green, and yellow colors). In the vegetated area, a litter cover and surface layers provide additional closely spaced (and superimposed) interfaces. These materials weaken the contrast in dielectric properties and make the air/soil interface more gradational than over the barren cinders. Compared with the cinders, the soil surface in the vegetated area is less hard and dense. These factors are believed to be responsible for the differences in near-surface signal amplitudes observed between the barren and vegetated areas.

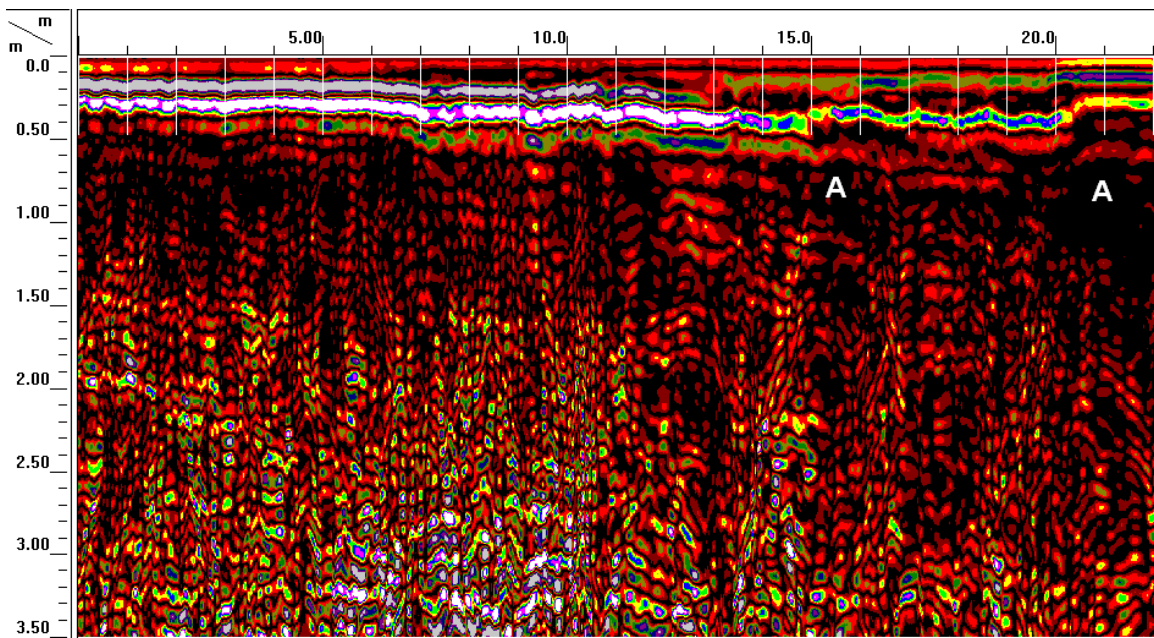


Figure 1. Radar record from Line 2 at the *Cinder Garden Site*.

The radar record shown in Figure 1 contains numerous subsurface point reflections. These point reflectors produce hyperbolic patterns. As suggested by Heggy et al. (2006), these reflectors may represent larger rock fragments or other heterogeneities within the cinders. While most reflectors appear to be chaotically arranged, there are faint linear patterns suggesting layering both beneath the barren and vegetated areas. These faint linear reflectors may represent slight differences in density or mineralogy produced by multiple eruptive events (Heggy et al., 2006). Several, poorly expressed layers dip downwards towards the right on this radar record. Reflections from these indistinct layers are partially obscured by reflections from the point reflectors. Beneath the vegetative area (distance marks 12 to 22-m), where the number of point reflectors is less, these planar reflections are more apparent. The number of point reflectors is less under the vegetated area than under the barren area. The reasons for this difference are unclear, but reverberation from the cinders located in surface layers of barren areas is suspected.

Within the vegetated area, in the upper part (40 to 130 cm) of the radar record, weak planar reflectors suggest soil horizons. In Figure 1, the letter “A” signifies areas in which the radar signal has been attenuated by the vegetation. Vegetation cycles nutrients (which accumulate in the soil) and presumably has greater moisture contents than the soil. These factors contribute to the attenuation of the radiated radar energy. The attenuation of the radar signal results in a zone of no signal return beneath the vegetation.

Figure 2 is a 20-m portion of traverse line 8 at the *Cinder Garden Site*. This record was obtained with the 400 MHz antenna. In Figure 2, all scales are in meters. The first 12-m of this traverse was conducted across a cinder barren. A vegetated area was entered near the 12-m mark and extends to the end of the traverse line. Once again, high and moderate amplitude surface reflections respectively distinguish barren from vegetated areas. In addition, the number of subsurface point reflectors appears greater beneath barren than vegetated areas. These reflectors may represent reverberations from cinders at or near the soil surface in barren areas and the dampening effect of soil layers in vegetated areas.

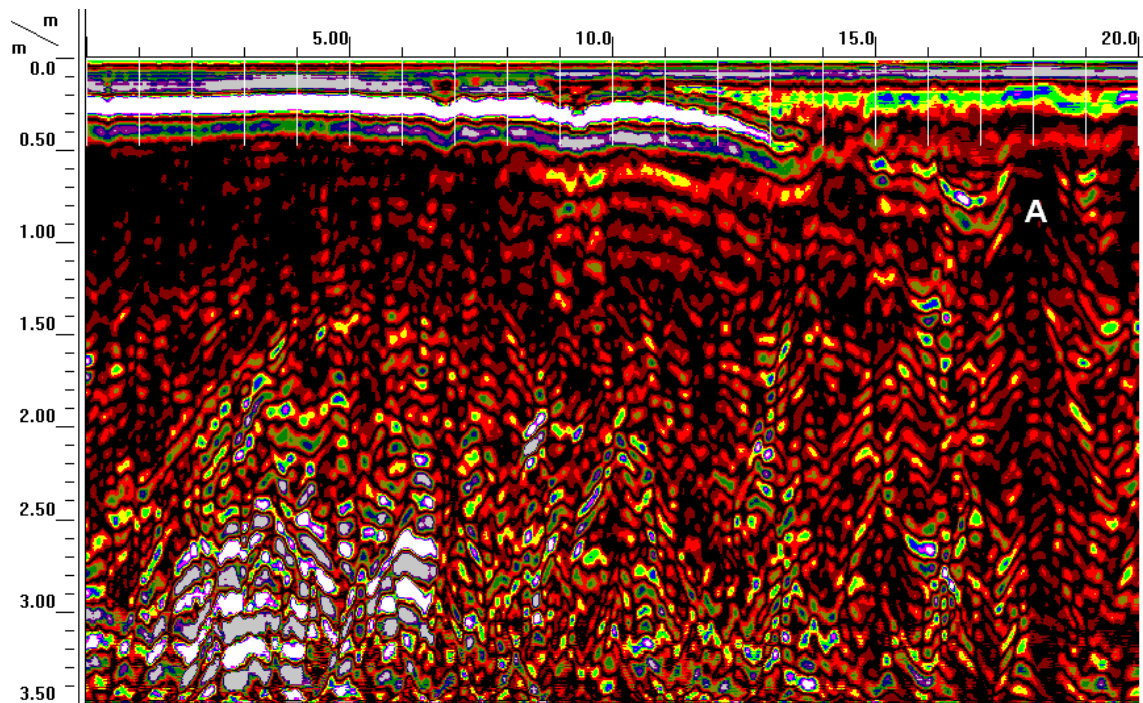


Figure 2. Radar record from Line 8 at the *Cinder Garden Site*.

Patterns of subsurface reflections are similar along GPR traverse line 8 (Figure 2) as they are along traverse line 2 (Figure 1), and all other traverse lines from the *Cinder Garden Site*. In the upper part of radar records, areas of barren cinders have higher amplitude surface reflections and reverberated signals than vegetated areas. Vegetated areas have moderate amplitude surface reflections. In addition, vegetated areas have several near-surface reflections that appear superimpose. These identifiable features are related to the presence of organic matter and soil horizons with some fines in vegetated areas. With the 400 MHz antenna, chaotic patterns of point reflectors are evident beneath all portions of the traverse lines. While point reflectors display a chaotic pattern, faint linear reflectors appear beneath both barren and vegetated areas. These faint linear reflectors are believed to represent stratigraphic layers of cinders of different grain sizes and/or density. However, higher amplitude reflections are evident in the lower part (generally below a depth of 250 cm) of radar records collected over barren areas than vegetated areas. This difference is attributed, in part, to the “*topographic roughness*” of the cinders and its effect on the antenna’s radiation pattern, antenna coupling, and scattering losses (Lampe and Holliger, 2003). In addition, this difference may be attributed at greater attenuation losses in surface layers of vegetated areas cause by the accumulation of organic materials (cycling of nutrients) and the development of soils (higher clay and moisture contents). It could also be attributed to more contrasting subsurface materials. In some areas, where the radar antenna passed directly over plants, increased attenuation of the radar signal resulted in a zone of no signal return beneath the vegetation. In my opinion, differences in many of the reflection patterns observed on radar records are the consequences of the growth of pioneering plants and the incipient development of soils.

Figure 3 is a 14.5-m portion of traverse line 3 at the *Service Road Site*. This record was obtained with the 400 MHz antenna. In Figure 3, all scales are in meters. The first 11-m of this traverse was conducted across barren cinders. A vegetated area was entered near the 11-m mark and extends to the end of the traverse line. Once again, differences in the amplitudes of surface reflections distinguish barren from vegetated areas. Most of the characteristic radar reflection signatures, which were discussed in the preceding paragraphs for the *Cinder Garden Site*, are repeated, with one exception at *Service Road Site*. A high amplitude, linear reflector occurs beneath the barren cinder area between depths of about 120 to 160 cm. This reflector represents an ashy layer. This layer was present on all radar records from the *Service Road Site*. This layer has presumably a higher available nutrient content and water storage capacity than the cinders. The subsurface layer of ash should be

more hospitable and inviting to plant growth and succession. However, at the *Service Road Site*, reflections from this layer were only evident beneath areas of barren cinders and not beneath vegetated areas. This suggests that the initial colonization of plants on cinders is more dependent on highly favorable surface or near-surface rather than subsurface conditions.

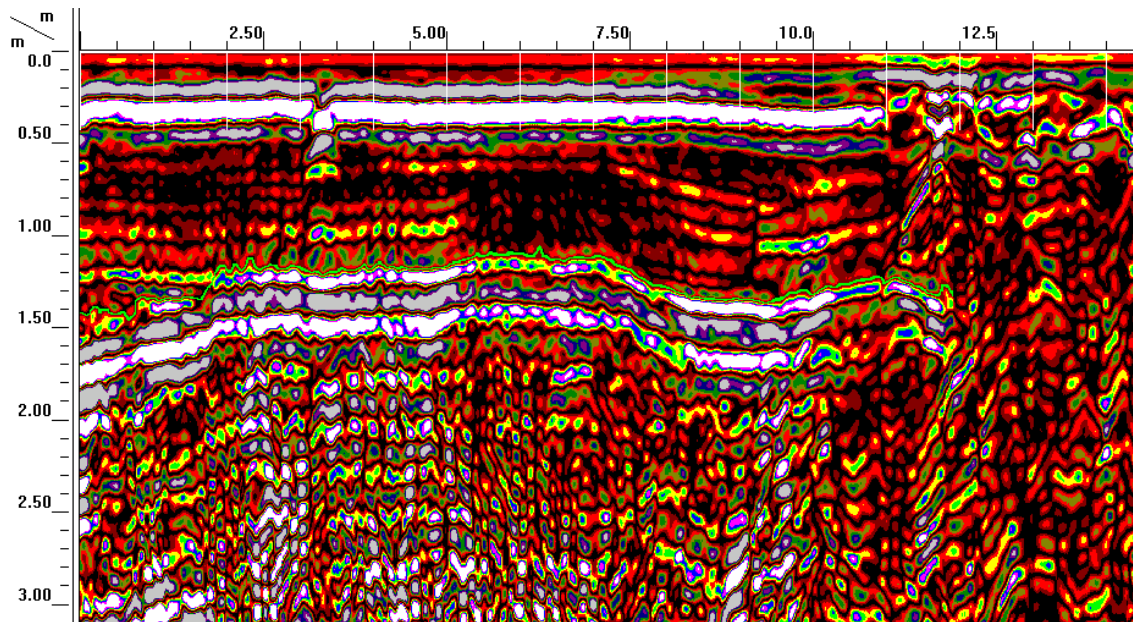


Figure 3. Radar record from Line 3 at the *Service Road Site*.

EMI Survey of the Cinder Garden Site:

Figure 4 shows spatial patterns of apparent conductivity (EC_a) measured with the EM38DD meter in the shallower-sensing, horizontal dipole (upper plot) and the deeper-sensing, vertical dipole (lower plot) orientations. In each plot, the isoline interval is 3.0 mS/m. In general, values of EC_a are very low and invariable across the Cinder Garden Site. This was expected, as cinders are electrically resistive and the soil mantle, where present, is relatively thin and has low clay, moisture, and soluble salt contents. Unfortunately, in areas of low conductivity, calibration error, signal drift, and background noise from spherics and cultural sources are more apparent in EC_a plots. This often results in spurious spatial patterns. Because of the electrically resistive nature of the cinders, background noise and signal interference are more noticeable than in areas of more conductive materials where EC_a plots typically have larger isoline intervals, which that hide these minor (1 to 2 mS/m) fluctuations.

In Figure 4, red dots have been used to show the general boundary of enclosed vegetated areas. Areas outside this boundary are mostly barren cinders. However, in some areas, this boundary was difficult to define as transition zones or vegetal outliers exist. In general, areas within the vegetative zones have higher EC_a in the shallower-sensing, horizontal dipole orientation (upper plot) and lower EC_a in the deeper-sensing, vertical dipole orientation (lower plot). While exceptions can be noted, the higher EC_a measurements obtained in the shallower-sensing, horizontal dipole orientation within the vegetated area can be attributed to the presence of an organic mat and the inferred higher moisture and clay contents of surface layers. No explanation for the lower EC_a in the deeper-sensing vertical dipole orientation is possible at this time. However, it was observed that operators raised the EM38DD meter to pass over plants within vegetative areas. It is reasonable, that this added air column caused a slight reduction in EC_a measurement collected in both dipole orientations.

Based on 1702 observations at the *Cinder Garden Site*, EC_a decreases and becomes less variable with increasing depth of observation. This relationship is attributed to the thin mantle of soil within the vegetated areas. The

mantle has higher organic matter, clay, and moisture contents than the cinders. In the shallower-sensing (0 to 75 cm) horizontal dipole orientation, EC_a averaged 4.8 mS/m with a standard deviation of 2.2 mS/m. At one-half of the observation points, the measured EC_a was between about 3.4 and 6.4 mS/m in the horizontal dipole orientation. In the deeper-sensing (0 to 150 cm) vertical dipole orientation, EC_a averaged 3.8 mS/m with a standard deviation of 1.4 mS/m. At one-half of the observation points, the measured EC_a was between 2.8 and 4.8 mS/m in the vertical dipole orientation.

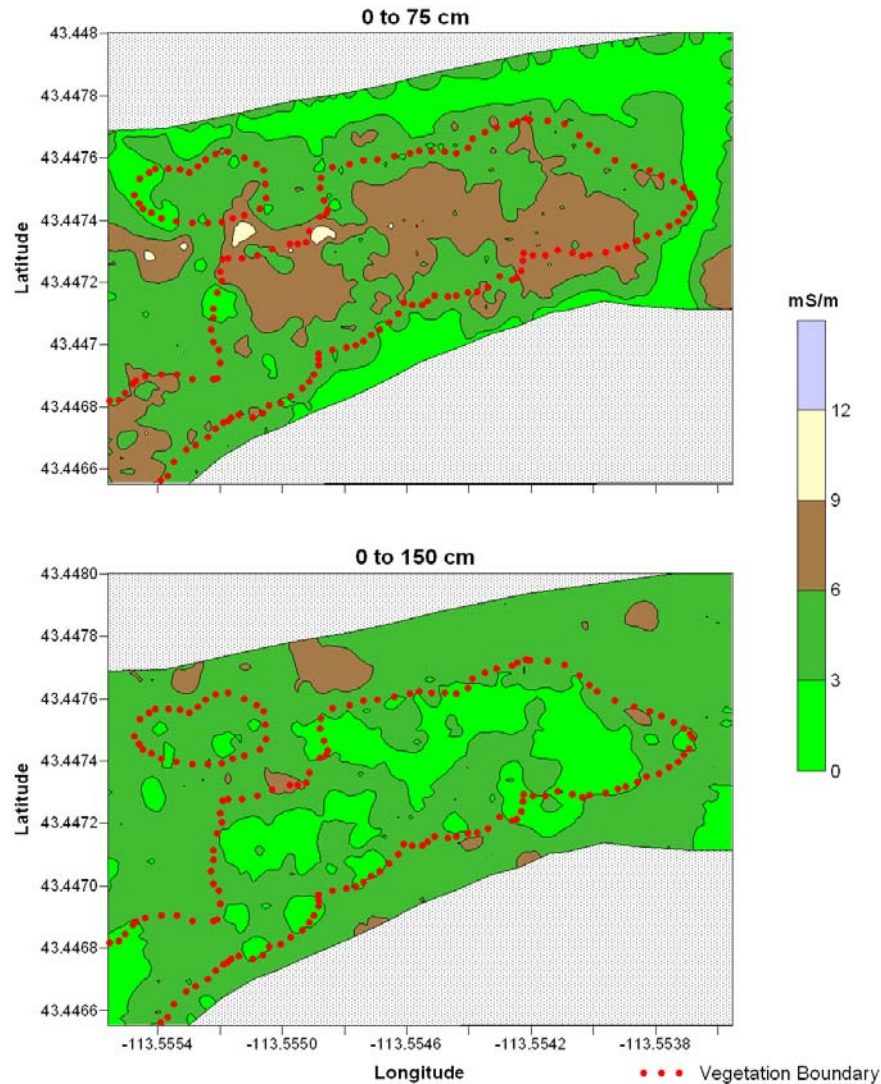


Figure 4. Spatial patterns of apparent conductivity measured with the EM38DD meter within the Cinder Garden Site.

GPR Survey at Laidlow Park, Craters of the Moon National Monument and Preserve:

Unsuccessful GPR surveys were conducted in an area of Deerhorn-Rehfield-Rock Outcrop complex, 2 to 15 percent slopes (MU 9) in an area known as Laidlow Park (43.26252 N. Lat., 113.65770 W. Long.). The moderately deep to duripan, well drained Deerhorn and the deep and very deep well drained Rehfield soils formed in aeolian deposits reworked by water over basalt. Deerhorn is moderately deep and Rehfield is deep and very deep to basalt bedrock. Deerhorn and Rehfield soils have argillic horizons with clay contents that

range from 18 to 30 percent. Deerhorn soil has high calcium carbonate content. Deerhorn is a member of the fine-loamy, mixed, superactive, mesic Argiduridic Durixeroll family. Rehfield is a member of the fine-loamy, mixed, superactive, mesic Ultic Argixeroll family. These soils are considered to have low potential for GPR.

Based on the measured depth (40 cm) to a buried reflector, the velocity of pulse propagation through the surface layers was an estimated 0.139 m/ns. The E_r was 4.6.

Figure 5 is an 8-m portion of traverse line that was conducted in an area of Deerhorn-Rehfield-Rock Outcrop complex, 2 to 15 percent slopes. Because of dense vegetation, the radar traverse was conducted along a dirt access road. The soil materials along the access road were heavily compacted and difficult to dig in. The radar record shown in Figure 5 was obtained with the 200 MHz antenna. In Figure 5, all scales are in meters. A white line has been used to approximate the depth to a subsurface interface believed to grade laterally into and out of both the duripan and bedrock. Basalt bedrock was observed to outcrop between 7 and 8 m distance marks on this radar record. In most areas where the bedrock was deeper than 100 cm, it was indiscernible.

The radar record shown in Figure 5 is considered extraordinary in terms of penetration depth and resolution of subsurface interfaces. In other area traversed with GPR, radar records were more depth restricted and provided little meaningful information.

In general, the radar records from areas of Deerhorn and Rehfield soils were depth restricted and suffered from low signal to noise ratios. The bedrock interface was difficult to identify and trace laterally. It is uncertain whether GPR detected the duripan. Because the depth of penetration is less than 100 cm and radar imagery is ambiguous, the use of GPR on these and similar soils is considered inappropriate for most soil survey applications.

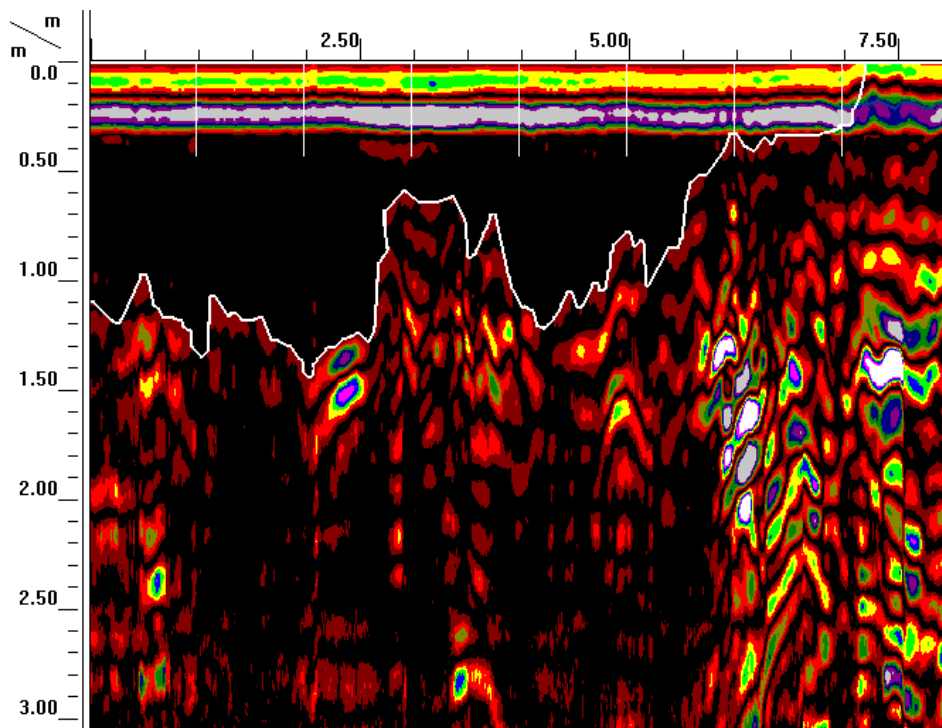


Figure 5. Radar record from an area of Deerhorn-Rehfield-Rock Outcrop complex, 2 to 15 percent slopes.

Saint Anthony Dune Field:
Background:

The penetration depth of GPR is dependent on the conductivity of the earthen materials being probed (Daniels, 2004). Soils with high electrical conductivity rapidly attenuate the radar signal and reduce penetration depths. The electrical conductivity of soils is highly variable and increases with increased water, clay, and soluble salt contents. It is significant that only relatively small amounts of water, clay, or soluble salts can noticeably increase the conductivity of soils and decrease the radar's depth of penetration.

In excessively drained, sandy soil materials, GPR often achieves unsurpassed penetration depths and unmatched resolution of subsurface interfaces. In these materials, lowering the frequency of the antenna can substantially increase penetration depths. As a consequence, little consideration is given to the chemical and physical properties of sandy materials. In sandy soils, the most significant form of signal loss is related to the presence of saline pore waters and surface reactive clays (Schenk et al., 1993). The presence of even small amounts of clay will significantly reduce the depth of penetration. In addition, mineralogical properties such as the concentration of heavy minerals affect the dielectric and magnetic properties and can have deleterious effects on GPR performance. In some areas (though especially in arid and semi-arid areas), high levels of calcium carbonate occur in soils. Soils with calcareous layers have been reported to severely limit the radar's depth of penetration (Grant and Schultz, 1994).

An on-going study is being conducted by the National Soil Survey Center to assess the chemical and mineralogical properties of sandy aeolian deposits that affect GPR performance. The Saint Anthony Dune Field provided an ideal site to collect data for this study.

Study Site:

The Saint Anthony Dune Field covers about 175 square miles and is located in the general vicinity of the town of St. Anthony. This dune field is about 5 miles wide, 35 miles long, and trends in a northeast direction (Alt and Hyndman, 1998). The sands consists "mostly of white quartz slightly peppered with occasional grains of black basalt" (Alt and Hyndman, 1998). Fragments of basalt and basalt bedrock are exposed in some interdune areas (see Figure 6). The study site is located to the immediate north of the *Egin Lakes Access* to the Saint Anthony Dunes Recreational Area (near 43.96712 N. Lat., 111.85439 W. Long.). The area is mapped as Dune Land (MU 17) (<http://websoilsurvey.nrcs.usda.gov>). These aeolian deposits contain as much as 1 % clay. These sandy aeolian deposits are well suited to GPR.



Figure 6. The Saint Anthony Dune Field.

Field Procedures:

A 40-m traverse line was established across a south-facing slope of a low dune on the border of the Saint Anthony Dune Field. The GPR traverse line extended from the crest of the dune to its foot slope. Survey flags were inserted in the ground at intervals of 1-m and served as reference points. The elevation of each reference point was measured with a level and stadia rod. Along the traverse line, relief was about 5.6 m. Elevations were not tied to a benchmark; the lowest recorded point was chosen as an arbitrary 0.0 m datum. The GPR survey was completed with a 200 MHz antenna.

Based on the measured depth (50 cm) to a buried reflector, the velocity of propagation through the upper part of the sands was an estimated 0.138 m/ns. The E_r was 4.67. Using a scanning time of 110 ns, a velocity of 0.138 m/ns, and equation [1], the maximum depth of penetration through the unsaturated sands is about 7.6 m. However, as shown in equation [2], the velocity of propagation is principally governed by the E_r of the profiled material(s), which will vary spatially and vertically with changes in water content. As a consequence, the depth scale shown in Figure 7 should be considered only a close approximation of the actual depth.

Results:

Figure 7 is the radar record from a low dune within the Saint Anthony Dune Field. In Figure 7, the surface has been *terrain corrected* to improve the visual presentation. Through a process known as *surface normalization*, elevations are assigned to each reference point and the image is corrected for changes in elevation. Surface normalization helps to improve the interpretative quality of radar records and the association of subsurface reflectors with landscape components.

The radar record obtained with the 200 MHz antenna is of good interpretive quality (see Figure7). The depth of penetration varied from about 7.0 m on the dune crest (reference point 0-m) to less than 1.2 m on the toe slope (reference point 40-m). Differences in the depth of penetration are attributed to changes in soil water content with landscape position. The ground water was assumed to have a comparatively high specific conductance, which would increase attenuation and limit the depth of penetration.

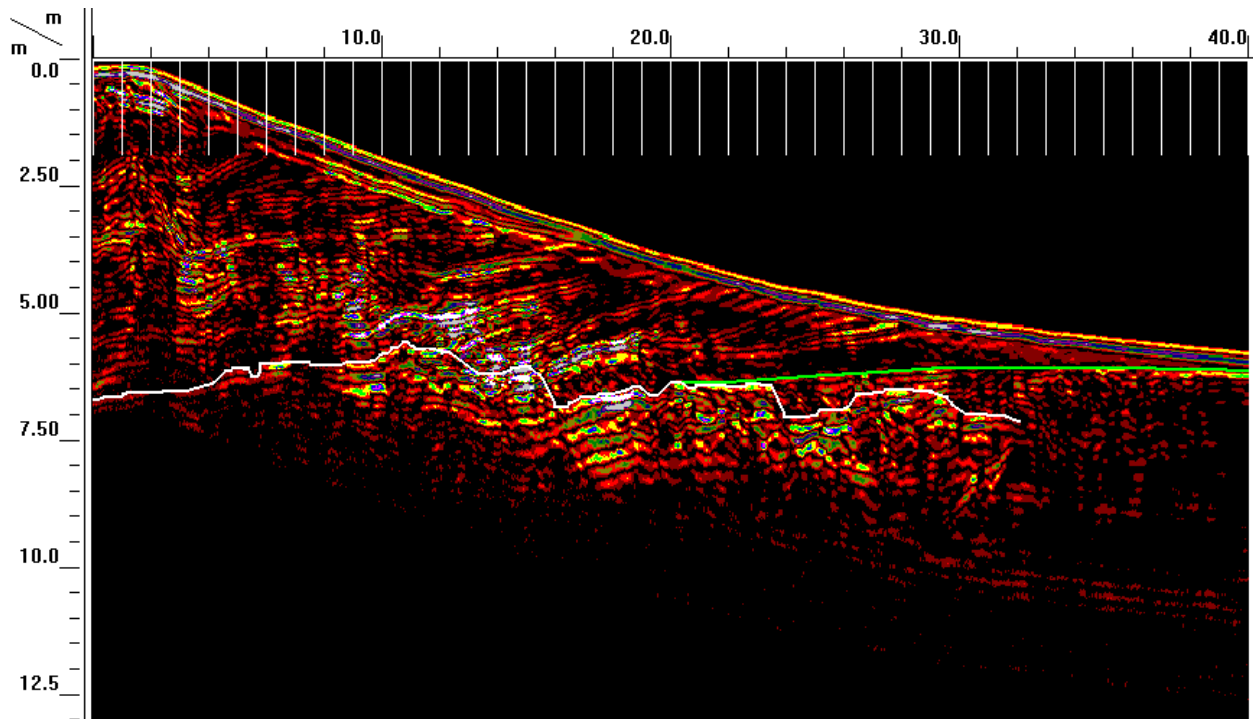


Figure 7. Radar record of a south-facing slope of a dune at the Saint Anthony Dune Field.

The internal geometry and structure of major stratigraphic boundaries within the dune are well expressed on this radar record (Figure 7). Abrupt and contrasting differences in density, grain size, and moisture contents produce the high amplitude reflections that are evident on this radar record. Beneath the crest and shoulder slope (reference marks 0 to 6-m) and within the upper 4-m of the profile, major flexures in bedding planes are evident. The inferred water table has been highlighted with a green-colored line in the right-hand portion of this radar record. Surface waters (Egin Lake) were observed a short distance from the toe slope end of the radar traverse line. The green line identifies a rather smooth and continuous reflector that dips slightly beneath the dune. The shallow depth of the water table and the general absence of subsurface reflections beneath this interface suggest attenuation losses caused by the presumably high specific conductance of the water. Though not verified, an irregular interface has been crudely approximated with a white-colored line. The irregular boundary and variable amplitudes of this interface suggests bedrock. In the right-hand portion of this radar record (between reference marks 30 and 40-m), multiples of the surface reflection clutter the lower part of the radar record (below about 6 m).

References

- Alt, D. D. and D. W. Hyndman, 1998. *Roadside Geology of Idaho*. Mountain Press Publishing Company, Missoula, MT.
- Daniels, D. J., 2004. *Ground Penetrating Radar; 2nd Edition*. The Institute of Electrical Engineers, London, United Kingdom.
- Gilbert, J. S., M. V. Stasiuk, S. J. Lane, C. R. Adam, M. D. Murphy, R. S. J. Sparks and J. A. Naranjo, 1996. Non-explosive, constructional evolution of ice-filled caldera at Volcan Sollipulli, Chile. *Bulletin of Volcanology*, 58: 67-83.
- Gomez-Ortiz, D., S. Martin-Velázquez, T. Martin-Crespo, A. Márquez, J. Lillo, I. López, and F. Carreno, 2006. Characterization of volcanic materials using ground-penetrating radar: A case study at Teide volcano (Canary Island, Spain). *Journal of Applied Geophysics* 59: 63-78.

- Geonics Limited. 2000. EM38DD ground conductivity meter: Dual dipole version operating manual. Geonics Ltd., Mississauga, Ontario.
- Grant, J. A. and P. H. Schultz, 1994. Erosion of ejecta at Meteor Crater: Constraints from ground penetrating radar. In: Proceedings Fifth International Conference on Ground-Penetrating Radar. Waterloo Centre for Groundwater Research and the Canadian Geotechnical Society. June 12 – 14, 1994, Kitchner, Ontario, Canada, pp.789-803.
- Grimm, R. E., R. Heggy, S. Clifford, C. Dinwiddie, R. McGinnis, D. Farrell, 2006. Absorption and scattering in ground-penetrating radar: Analysis of the Bishop Tuff. *Journal of Geophysical Research*, Volume III E06S02: 1-15.
- Heggy, E., S. M. Clifford, R. E. Grimm, C. L. Dinwiddie, D. Y. Wyrick, B. E. Hill, 2006. Ground-penetrating radar sounding in mafic lava: Assessing attenuation and scattering losses in Mars-analog volcanic terrains. *Journal of Geophysical Research*, Volume III E06S04: 1-16.
- Lampe, B. and K. Holliger, 2003. Effects of fractal fluctuations in topographic relief, permittivity and conductivity on ground-penetrating radar antenna radiation. *Geophysics* 68(6): 1934-1944.
- McCoy, F. W., S. Papmarinopoulos, C. Dumas, and C. Palyvou, 1992. Probing the Minoan eruption on Thera with ground-penetrating radar: buried extent of Akrotiri, tephra stratigraphy and late Bronze Age volcanic hazards. Geological Society of America, 1992 Annual Meeting, Abstracts with Programs 24:26.
- Miyamoto, H., J. Haruyama, S. Rokugawa, K. Onishi, T. Toshioka, J-I Koshinuma, 2003. Acquisition of ground-penetrating radar data to detect lava tubes: preliminary results on the Komorian Cave at Fuji Volcano in Japan. *Bull. Eng. Geol. Env.* 62: 281-288.
- Olhoeft, G. R. D. B. Sinex, K. A. Sander, M. M. Lagmanson, D. E. Stillman, S. Lewis, B. T. Clark, E. L. Wallin and J. P. Kauahikaua, 2000 . Hot and cold lava tube characterization with ground penetrating radar. 482-487 pp. In: Proceedings - SPIE - The International Society of Optical Engineering.
- Paillou, P., G. Grandjean, J-M. Malezieux, G. Ruffie, E. Heggy, D. Piponnier, P. Dubois, and J. Achache, 2001. Performances of ground penetrating radar in arid volcanic regions: consequence for Mars subsurface exploration. *Geophysical Research Letters* 28(5): 911-914.
- Russell, J. K. and M. V. Stasiuk, 1997. Characterization of volcanic deposits with ground-penetrating radar. *Bulletin of Volcanology* 58: 515-527.
- Russell, J. K. and M. V. Stasiuk, 2000. Ground-penetrating radar mapping of Minoan volcanic deposits and the Late Bronze Age palaeotopography, Thera, Greece. 105-121 pp. IN: McGuire, W. J., D. R. Griffiths, P. L. Hancock and I. S. Stewart (editors.). *The Archaeology of Geological Catastrophes*. The Geological Society of London, Special Publications, 171. London, UK.
- Rust, A. C. and J. K. Russell, 2001. Mapping porosity variation in a welded pyroclastic deposit with signal and velocity patterns from ground-penetrating radar surveys. *Bulletin of Volcanology* 62: 457-463.
- Schenk, C. J., D. L. Gautier, G. R. Olhoeft, and J. E. Lucius. 1993. Internal structure of an Aeolian dune using ground-penetrating radar. *Special Publications Int. Association of Sedimentology* 16: 61-69.
- Shapiro, S., L. Brown, and T. Tchakirides, 2005. GPR imaging of lava flows on Hawaii. *Geophysical Research Abstracts* Vol. 7, 10550.